Association of Metallurgical Engineers of Serbia *Scientific paper*
AMES *UDC: 669.018.9:[669.721+669.6*

STUDIES OF Mg_2Sn-BASED COMPOSITES

Varužan Kevorkijan[1*], Srečo Davor Škapin[2]

[1]*Independent Researcher, Betnavska cesta 6, 2000 Maribor, Slovenia*
[2]*Srečo Davor Škapin, Institute Jozef Stefan, Jamova 39, 1000 Ljubljana, Slovenia*

Received 28.02.2010
Accepted 23.03.2010.

Abstract

Single phase Mg_2Sn powders were successfully reaction-synthesized from the elements and applied for the preparation of Mg_2Sn-based composites of different nature, microstructure and combination of properties. These were fully dense (≥95 % T.D.) Mg- and Al-metal matrix composites (MMCs) reinforced with either Mg_2Sn particles or mixtures of Mg_2Sn with TiC or TiB_2 particulates by infiltration of porous Mg_2Sn preforms with molten magnesium or aluminium; and (ii) Mg_2Sn intermetallic matrix composites (IMCs) discontinuously reinforced with TiC and TiB_2 particles by pressureless sintering. The microstructures of the composite samples were examined using scanning electron microscopy (SEM-EDS) and X-ray powder diffraction (XRD). The mechanical properties were evaluated by Vickers hardness measurements performed at room temperature, while the fracture toughness of the specimens was determined by applying the indentation method. Based on the data accumulated, an evaluation of the mechanical properties of these composites on the basis of the volume content of different constituents was performed. Moreover, the ability of various microstructures obtained by pressureless infiltration and sintering for tailoring the desired combination of mechanical properties. (e.g. toughening in combination with hardness) was also investigated and reported. Thus, the infiltration led to MMCs with different microstructures and mechanical properties, depending on the infiltrant applied. The samples infiltrated with molten magnesium possessed characteristic lamellar ("Chinese script") eutectic microstructure and thereby an enhanced fracture toughness (up to 7.7 $MPa \cdot m^{1/2}$ in non-reinforced and 5.8 $MPa \cdot m^{1/2}$ in reinforced counterparts), and in combination with Vickers hardness were superior to those of conventional Mg-Sn alloys. On the other hand, although the mechanical response (Vickers hardness) of samples infiltrated with aluminium was even better than in counterparts infiltrated with magnesium, the absence of the "Chinese script" microstructure was observed to have a

* Corresponding author: Varužan Kevorkijan varuzan.kevorkijan@impol.si

detrimental influence on fracture toughness, which was significantly lower in these samples. The densification of Mg_2Sn matrix discontinuously reinforced with TiC or TiB_2 ceramic reinforcement performed by a non-reactive, solid-state sintering, resulted in samples with high density (≥95% T.D.) and different combinations of mechanical properties compared to MMCs obtained by infiltration. The Vickers hardness of sintered IMCs were much higher than in MMCs obtained by infiltration, with the exception of the fracture toughness which was reduced below 1.8 $MPa \cdot m^{1/2}$.
Key words: Mg_2Sn, composites, reinforcement, TiC, TiB_2

Introduction

Current applications of magnesium stannide (Mg_2Sn) are limited to optimisation of the microstructure and mechanical properties of magnesium [1-7] and in lead-free aluminium alloys [8]. In Mg-Sn and Mg-Sn-Ca creep resistant magnesium alloys, Mg_2Sn precipitates are applied as a thermally stable intermetallic phase for suppressing grain boundary sliding and dislocation movement, resulting in an improvement of creep properties.

However, due to its melting point (770 °C) higher than magnesium, relatively low density (3.59 g/cm^3 - about half that of the density of tin), excellent compressibility ($2.83 \cdot 10^{-11}$ m^2/N, approx. 50% higher than for Mg_2Si) and a thermal expansion coefficient ($9.9 \cdot 10^{-6}$ K^{-1}) similar to some borides and carbides [9, 10], magnesium stannide is a promising structural material, particularly in combination with magnesium and aluminium alloys and composites. The Vickers hardness of Mg_2Sn is about 1.2 GPa [7], significantly lower than for Mg_2Si (3.5-7.0 GPa), but still twice as high in comparison with the hardness of Mg-Sn alloys.

In addition, Mg_2Sn is a line compound suitable for achieving characteristic eutectic microstructures (i.e. "Chinese-scipt") and therefore for tailoring the properties of composites (particularly fracture toughness) with Mg_2Sn appearing as a matrix or a reinforcement phase.

In contrast to numerous investigations carried out in developing Mg-Sn alloys with Mg_2Sn precipitates formed *in situ*, only a limited number of investigations were concerned with the synthesis of Mg_2Sn powder [11] and, according to our knowledge, none with its densification, alone or with some other reinforcing phases, i.e. as a matrix for high temperature composites or as particulate reinforcement in metal matrix composites.

Hence, in the present study, the following investigations were performed in order to demonstrate the potential of Mg_2Sn as an advanced composite matrix or discontinuous reinforcement: (i) synthesis of Mg_2Sn single phase powder from the elements; (ii) pressureless sintering and characterisation of Mg_2Sn-based intermetallic matrix composites discontinuously reinforced with TiC or TiB_2 particles, and (iii) formation and characterisation of Mg- or Al-metal matrix composites reinforced with either Mg_2Sn particles or mixtures of Mg_2Sn with TiC or TiB_2 particulates by infiltration of porous Mg_2Sn preforms with molten magnesium and aluminium.

Experimental procedure

In the first part of the experimental work, Mg_2Sn powder was synthesized by reaction synthesis from the elements. As the source of magnesium and tin, cylindrical samples machined from pure magnesium and tin rods (supplier: ESPI) were used. Magnesium and tin samples in three different molar ratios (stoichiometric, with 5 mol.. % and 10 mol. % excess of magnesium) were placed in a platinum crucible and heated in a vacuum furnace (for 2 h at 660 °C or for 1h at 700 °C) in a static atmosphere of argon. This was followed by cooling to room temperature and characterisation of the as-obtained product by optical and scanning electron microscopy (OM and SEM, respectively) and X-ray diffraction (XRD). After that, the product was subsequently milled in an attrition mill for various milling time (0.5-2 h) in order to achieve the desired morphology of Mg_2Sn particles. The as-milled Mg_2Sn powders were then applied for various infiltration and sintering experiments.

Infiltration was performed by using porous preforms made of laboratory synthesized Mg_2Sn powder of grade C (Table 1) and mixtures of Mg_2Sn powder grade C and commercially available TiC (99.5%, d_{50} = 4 μm) and TiB_2 powders (99.5%,d_{50} = 6 μm), as listed in Table 2. Preforms were isostatically pressed under various pressures (from 80 to 150 MPa) in order to achieve samples with different porosity.

Table 1: Phase composition and morphology of laboratory prepared Mg_2Sn powders

Powder	Mg_2Sn (vol. %)	Sn (vol. %)	d_{50} (μm)
Grade A	95	5	3.3
Grade B	97	3	2.4
Grade C	99.8	0.2	2.1

Table 2: The composition of various Mg_2Sn-TiC and Mg_2Sn-TiB_2 mixtures used for preforms preparation in infiltration experiments

Mixture	Initial composition
#1	100 vol. % Mg_2Sn (grade C)
#2	75 vol. %Mg_2Sn (Grade C)–25 vol. %TiC
#3	75 vol. %Mg_2Sn (Grade C) -25 vol.%TiB_2
#4	70 vol. %Mg_2Sn (Grade C) -30 vol. %TiC
#5	70 vol. %Mg_2Sn (Grade C) –30 vol. %TiB_2

The samples obtained were cylinders 50 mm high and 20 mm in diameter. As infiltrant, Al-xSn and Mg-xSn (x=3%, 5%) alloys were applied. Al-xSn and Mg-xSn alloys necessary for infiltration were prepared from pure aluminium or magnesium and pure tin powders melted in a graphite crucible with the protection of a fusing agent. The melt was stirred to ensure homogeneity. Finally it was cast into a preheated mould. The as-cast ingots were cut and machined to thin cylinders having the same diameter as the Mg_2Sn preforms (20 mm). Finally, a preform sandwiched between two Al-xSn or Mg-xSn plates was placed in a ceramic crucible by the following procedure: the first Al-xSn or Mg-xSn plate was placed on the bottom of crucible and the preform was fixed on it using upper and lower preformatted steel plates. After that, the upper Al-xSn or Mg-xSn plate was placed on it. The volume of the Al-xSn or Mg-xSn plates was calculated to be

approximately 50% higher than the volume of the pores in the preform. The infiltration was conducted by heating the assembly in a vacuum furnace at 730 °C for 1h, under a static atmosphere of argon.

After completion of the infiltration, the assembly was cooled to room temperature and the infiltrated preform was removed from the furnace.

Green samples for sintering experiments were formulated by blending the synthesized Mg_2Sn powder (grade C, Table 1) with commercial ceramic powders (TiC and TiB_2) in appropriate amounts to create intermetallic matrix composites (IMCs) with 10, 30 and 50 wt. % of TiC or TiB_2 reiforcement. The powder blends were thoroughly mixed in a planetary mill and subsequently cold compacted. In all cases, sintering of the compacts was conducted at 750 °C for 1 h in a static atmosphere of argon using a vacuum furnace.

The as-synthesized composite samples were cut, machined and polished in accordance with standard procedures.

Microstructural characterization of the fabricated composites was performed by OM and SEM, whereas XRD measurements were applied to the samples to identify the phases and their crystal structure.

Quantitative determination of the volume percentage of Mg_2Sn and ceramic particles in the matrix, as well as the retained porosity, was performed by analysing optical and scanning electron micrographs of polished composite bars using the point counting method and image analysis and processing software.

Composite density measurements were carried out using Archimedes' principle, applying absolute ethanol as the immersion fluid.

The initial density of the green compacts (preforms and tablets) was calculated from the mass and geometry of the samples.

Vickers hardness (HV) measurements were performed at room temperature on polished composite samples and calculated as the average of 6 indentations. These measurements were made with a conventional Vickers tester (load: 9.8-24.5 N; residence time: 15 s).

Due to their small dimensions and high brittleness, the fracture toughness of the specimens obtained was determined by applying the indentation method [12]. K_{IC} of the composite samples was determined from submicron derived indentation cracks and calculated according to the following equations proposed by Niihara et al. [13]:

$$((K_{IC}\Phi)/(Ha)^{1/2})\,(H/(E\Phi))^{2/5} = 0.035(L/a)^{-(1/2)} \quad (1.25 \leq c/a \leq 2.5) \qquad (1)$$

$$((K_{IC}\Phi)/(Ha)^{1/2})\,(H/(E\Phi))^{2/5} = 0.129(c/a)^{-(3/2)} \quad (c/a \geq 2.5) \qquad (2)$$

where H is the Vickers hardness, a and c are the length of the half diagonal of the indent and the length of the half indentation crack, respectively, L = c-a, E is Young's modulus, and Φ is a constant with a magnitude of about 3.

Results and discussion

Mechanism of the formation, chemical composition and morphology of laboratory prepared Mg_2Sn powder

Depending on the initial composition of the reaction mixture and the heating conditions, the concentration of Mg and Sn impurities in the synthesized Mg_2Sn phase varied significantly.

Applying reaction mixtures with a stoichiometric ratio of elemental magnesium and tin, more than 5 wt. % of tin remained in the reaction product obtained (Mg_2Sn powder grade A, Table 1), which was most probably caused by the loss of magnesium. This presumption was additionally confirmed by the experimental finding that the amount of non-reacted tin increased with increasing temperature of the synthesis.

On the other hand, by applying a reaction mixture with a slight (5 mol. %) excess of magnesium, the amount of non-reacted tin was reduced below 5 wt. % or even below 3 wt. % (grade B, Table 1) at a lower temperature of synthesis (660 °C).

Finally, by using a reaction mixture with 10 mol. % excess of magnesium, single phase Mg_2Sn (grade C, Table 1) with no Mg or Sn peak detected in the XRD pattern was prepared at 700 °C.

Investigation of the solidified product samples indicated that the reaction mechanism of Mg_2Sn synthesis is homogeneous nucleation and growth. Based on the phase diagram of the Sn-rich corner in the Mg-Sn binary system [14], it is evident that Mg will start to dissolve into the liquid phase immediately after the temperature exceeds the melting point of Sn (505 K). With increasing temperature, a greater amount of Mg will be dissolved and, after melt saturation, Mg_2Sn will start to nucleate according to Eq.1:

$$Mg_{(s)} + Sn_{(l)} = Mg_2Sn_{(s)} \qquad (1)$$

Above the melting point of magnesium (923 K), the nucleation of Mg_2Sn will continue by nucleation from the saturated liquid phase according to the Eq. 2:

$$Mg_{(l)} + Sn_{(l)} = Mg_2Sn_{(s)} \qquad (2)$$

Thus, to achieve complete conversion of reactants into Mg_2Sn, it is important to preserve a permanent excess of magnesium (approx. 10 wt. %) in the system up to the end of the synthesis.

The morphology of laboratory prepared Mg_2Sn powder, obtained by milling the solidified sample from reactive synthesis, is presented in Fig. 1. As evident, the powder obtained is non-agglomerated, with well shaped individual particles of particle size mostly below 5 μm.

The typical phase composition in the synthesized Mg_2Sn powders is reported in Table 1. The composition of various Mg_2Sn-TiC and Mg_2Sn-TiB_2 mixtures used for preforms in infiltration experiments are listed in Table 2.

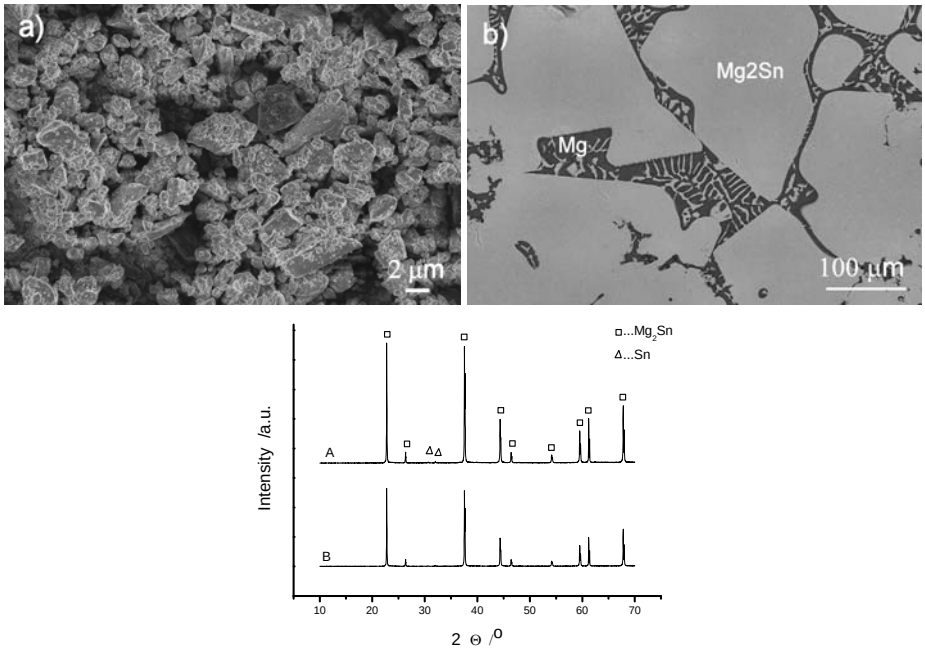

Fig. 1. a) SEM micrograph of Mg_2Sn powder (grade B) after milling, b) SEM micrograph of as-synthesized Mg_2Sn and b) X-ray powder diffraction pattern of the prepared compound Mg_2Sn: A – grade B powder (Table 1), and B – grade C powder (Table 1).

Al- $Mg_2Sn_{(p)}$ and Mg- $Mg_2Sn_{(p)}$ composites made by pressureless infiltration

Infiltration of porous Mg_2Sn preforms (composition #1, Table 2) with molten Al resulted in fully dense composite samples with a continuous aluminium-based matrix, reinforced with Mg_2Sn particles and Mg_2Sn precipitates appearing near the primary Mg_2Sn particles, Fig. 2a.

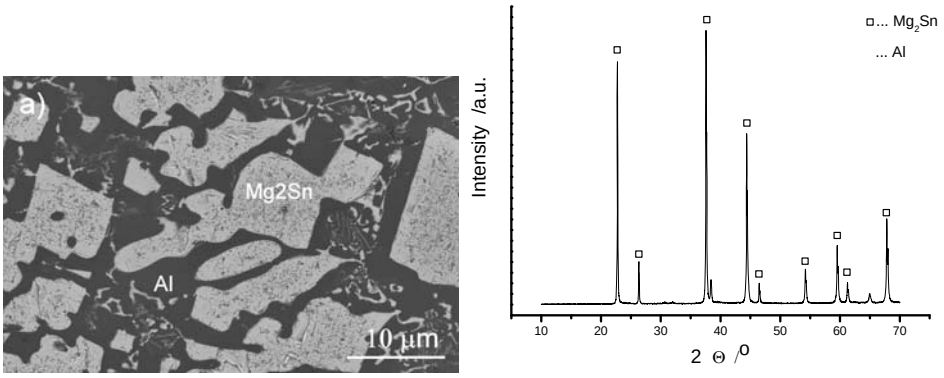

Fig. 2. a) SEM micrograph and b) X-ray powder diffraction pattern of the pressurelessly infiltrated Mg_2Sn-Al composite sample.

On the other hand, samples fully infiltrated with molten magnesium have a characteristic lamellar ("Chinese script") eutectic microstructure, Fig. 3a, and completely different mechanical properties, Table 3.

Table 3: Average room temperature Vickers hardness and fracture toughness of Al-Mg_2Sn composites prepared by pressureless infiltration

Composite composition (vol. %)	Retained porosity (vol. %)	Density (g/cm^3)	Vickers hardness (GPa)	K_{IC} ($MPa\ m^{1/2}$)
18% Al-82% Mg_2Sn	2.2±0.2	3.5±0.4	0.87±0.09	3.4±0.4
29% Al-71% Mg_2Sn	3.5±0.4	3.4±0.3	0.82±0.08	4.7±0.5
38% Al-62% Mg_2Sn	4.7±0.5	3.3±0.3	0.75±0.08	5.3±0.5
19% Al-81% Mg_2Sn	2.0±0.2	3.6±0.4	0.88±0.09	3.9±0.4
28% Al-72% Mg_2Sn	3.2±0.3	3.5±0.4	0.83±0.08	4.8±0.5
38% Al-62% Mg_2Sn	3.9±0.4	3.4±0.3	0.79±0.08	5.6±0.6

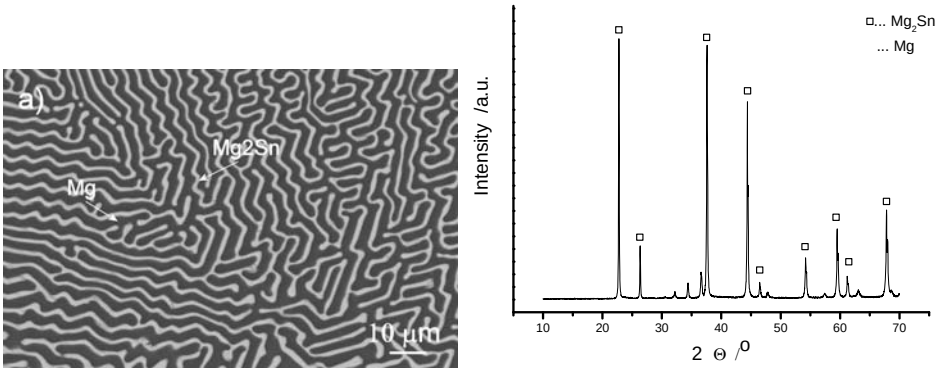

Fig. 3. a) SEM micrograph and b) X-ray powder diffraction pattern of the Mg_2Sn-Mg composite sample infiltrated at 730°C showing a lamellar structure consisting of Mg_2Sn »Chinese-script« in a matrix of magnesium

In both cases, due to the complete and non-reactive wetting of the Mg_2Sn preform skeleton with molten Mg or Al, the infiltration proceeded spontaneously, under atmospheric pressure. The absence of chemical reactions between the preform skeleton and the molten infiltrants was proved by the corresponding X-ray diffraction patterns, Figs. 2b and 3b.

As evident from Tables 3 and 4, Vickers hardness of Al-Mg_2Sn and Mg-Mg_2Sn MMCs are increasingly improved on increasing the amount of Mg_2Sn particulate reinforcement. However, regarding the fracture toughness, quite the opposite behaviour was ascertained. The fracture toughness of Al-Mg_2Sn and Mg-Mg_2Sn MMCs decreases with increase in the amount of Mg_2Sn particulates.

Table 4: Average room temperature Vickers hardness and fracture toughness of Mg-Sn-Mg_2Sn composites prepared by pressureless infiltration

Composite composition (vol. %)	Retained porosity (vol. %)	Density (g/cm^3)	Vickers hardness (GPa)	K_{IC} (MPa $m^{1/2}$)
20% Mg-80% Mg_2Sn	2.2±0.2	3.3±0.3	0.66±0.07	4.7±0.5
28% Mg-71% Mg_2Sn	3.5±0.4	3.1±0.3	0.72±0.07	6.5±0.7
41% Mg-59% Mg_2Sn	4.7±0.5	2.9±0.3	0.77±0.08	7.3±0.7
19% Mg-81% Mg_2Sn	2.0±0.2	3.4±0.4	0.61±0.06	5.4±0.5
31% Mg-69% Mg_2Sn	3.2±0.3	3.1±0.4	0.69±0.07	6.6±0.7
38% Mg-62% Mg_2Sn	3.9±0.4	3.0±0.3	0.71±0.07	7.7±0.8

Comparing the mechanical properties of Al-Mg_2Sn and Mg-Mg_2Sn MMCs, it is found that Vickers hardness is evidently higher in samples infiltrated with aluminium. However, the fracture toughness is an exception, becoming greater (almost doubled) in samples infiltrated with magnesium.

The extraordinary fracture toughness of Mg-Mg_2Sn MMCs is caused by their characteristic lamellar structure consisting of Mg_2Sn "Chinese script" in a matrix of magnesium solid solution.

Al-$Mg_2Sn_{(p)}$-$TiC_{(p)}$ and Al- $Mg_2Sn_{(p)}$-$TiB_{2(p)}$ composites made by pressureless infiltration

Preforms made from mixtures of laboratory synthesized Mg_2Sn powder and commercially available TiC and TiB_2 powders (compositions #1, #2, #3 and #4), were also successfully pressurelessly infiltrated with molten aluminium, resulting in samples with almost theoretical density and interesting combinations of mechanical properties.

The microstructure of infiltrated samples consisted of a co-continuous network of Mg_2Sn phase interpenetrated by an aluminium matrix with fine dispersed TiC or TiB_2 particles, Figs. 4 and 5. The absence of secondary phases, Fig. 5b, indicates that in this case spontaneous infiltration also proceeded as a non-reactive process.

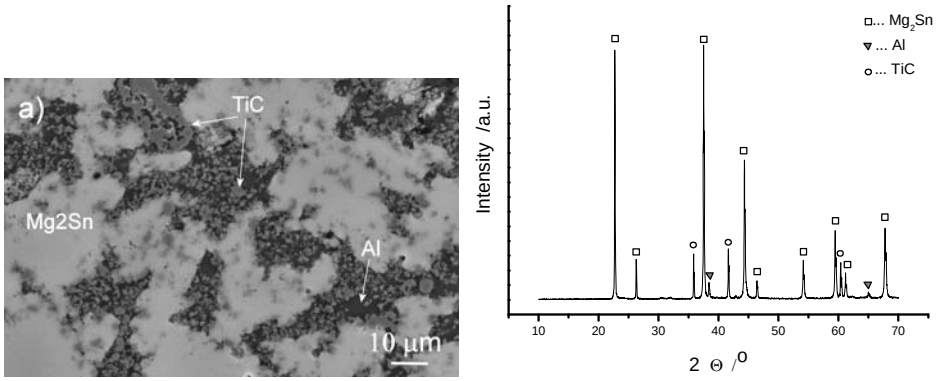

Fig. 4. a) SEM micrograph and b) XRD spectrum of pressureless infiltrated Al-Sn-$Mg_2Sn_{(p)}$-$TiC_{(p)}$ composite sample with an initial composition of the preform skeleton of 69 vol.% Mg_2Sn, 29 vol. % TiC and 2 vol. Al.

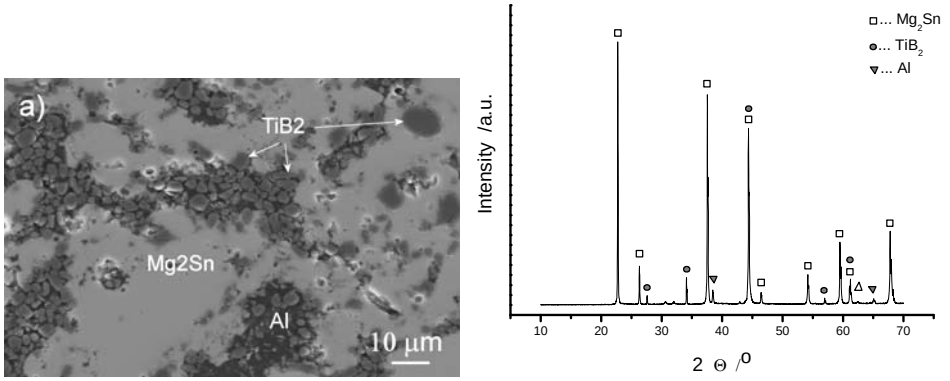

Fig. 5. a) SEM micrograph and b) XRD spectrumof pressurelessly infiltrated Al-Sn-$Mg_2Sn_{(p)}$-$TiB_{2(p)}$ composite sample with an initial composition of the preform skeleton 75 vol.% Mg_2Sn, 25 vol. % TiB_2.

Reinforcement of an Al matrix with TiC or TiB_2 particles resulted in a marked improvement of Vickers hardness. As evident from Table 5, the Vickers hardness of Al-Mg_2Sn-TiC and Al-Mg_2Sn-TiB_2 composites was approx. 50% higher than in non-reinforced Al-Mg_2Sn samples, Table 3.

Table 5: Average room temperature Vickers hardness and fracture toughness of Al-Sn-$Mg_2Sn_{(p)}$(grade C)-$TiC_{(p)}$ and Al-Sn-$Mg_2Sn_{(p)}$(grade A)-$TiB_{2(p)}$ composites prepared by pressureless infiltration

Composite composition (vol. %)	Retained porosity (vol. %)	Density (g/cm^3)	Vickers hardness (GPa)	K_{IC} ($MPa\ m^{1/2}$)
28% Al-48%Mg_2Sn -23 %TiC	1.9±0.2	3.6±0.2	1.29±0.13	2.8±0.3
36%Al-46%Mg_2Sn -18%TiC	2.2±0.2	3.5±0.2	1.14±0.11	3.1±0.3
28%Al-49%Mg_2Sn -23%TiB_2	3.5±0.4	3.6±0.2	1.38±0.14	2.7±0.3
35%Al-46%Mg_2Sn -19%TiB_2	4.7±0.5	3.5 ±0.2	1.26±0.13	3.0±0.3

Examination of the fracture toughness, Table 5, revealed that the toughness of MMCs was inversely proportional to the total amount of reinforcing phase. Moreover, it became lower by replacing some of the Mg_2Sn particles with more brittle TiC or TiB_2 particulates. This is well documented in Tables 3 and 5 for samples with approximately the same total amount of particulate reinforcement.

Mg -$Mg_2Sn_{(p)}$-$TiC_{(p)}$ and Mg-$Mg_2Sn_{(p)}$-$TiB_{2(p)}$ composites made by pressureless infiltration

Experiments showed that infiltration of Mg_2Sn-TiC and Mg_2Sn-TiB_2 preforms with molten magnesium proceeded spontaneously, without chemical reaction between the preform skeleton and molten magnesium. By adjusting the porosity of the preforms within the range of 30 to 35 vol. %, composites with different compositions listed in

Table 6 were routinely fabricated. At 900 °C, the infiltration was complete within 1h, resulting in composite samples with less than 5 vol. % of retained porosity.

Table 6: Average room temperature Vickers hardness and fracture toughness of Mg-$Mg_2Sn_{(p)}$-$TiC_{(p)}$ and Mg- $Mg_2Sn_{(p)}$ -$TiB_{2(p)}$ composites prepared by pressureless infiltration

Composite composition (vol. %)	Retained porosity (vol. %)	Density (g/cm^3)	Vickers hardness (GPa)	K_{IC} (MPa $m^{1/2}$)
29% Mg-47%Mg_2Sn-1%Al-23 %TiC	1.9±0.2	3.4±0.2	1.16±0.12	4.9±0.5
36%Mg-38%Mg_2Sn-7%Al–19%TiC	2.2±0.2	3.5±0.2	1.0±0.19	5.8±0.6
29%Mg-48%Mg_2Sn–1%Al-22%TiB_2	3.5±0.4	3.3±0.2	1.24±0.12	4.4±0.4
35%Mg-39%Mg_2Sn–7%Al-19%TiB_2	4.7±0.5	3.3±0.2	1.13±0.11	5.3±0.5

The resulting composite samples have a typical eutectic microstructure showing a lamellar structure consisting of Mg_2Sn "Chinese script" in a matrix of magnesium solid solution, additionally reinforced with fine TiC or TiB_2 particles, Fig. 6.

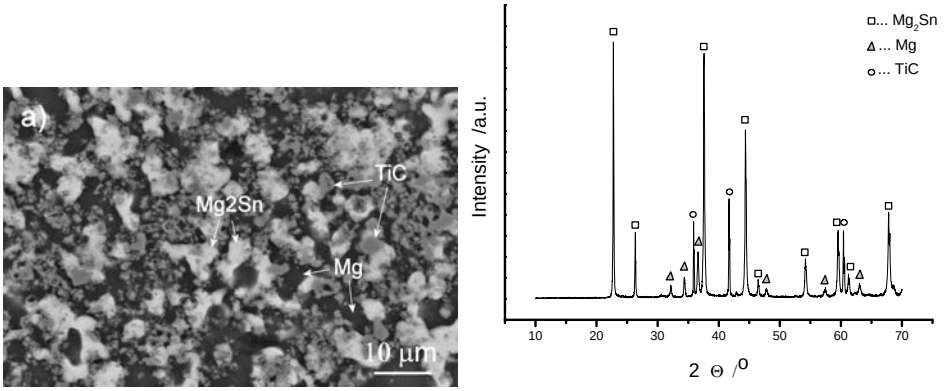

Fig. 6. a) SEM micrograph and b) XRD spectrum of Mg-Sn-$Mg_2Sn_{(p)}$-$TiC_{(p)}$ with an initial composition of the preform skeleton 70 vol.% Mg_2Sn and 30vol. % TiC.

From the X-ray diffraction patterns of the composite samples it is evident (Fig. 7b and 8b) that besides Mg_2Sn reinforcement and irrespective of matrix composition, no secondary phases were detected, which indicates that pressureless infiltration of Mg_2Sn preforms with molten Mg-Sn-based alloys was not chemically assisted. A detailed SEM examination of interface regions of all samples also confirmed the absence of chemical reactions between the composite constituents listed above.

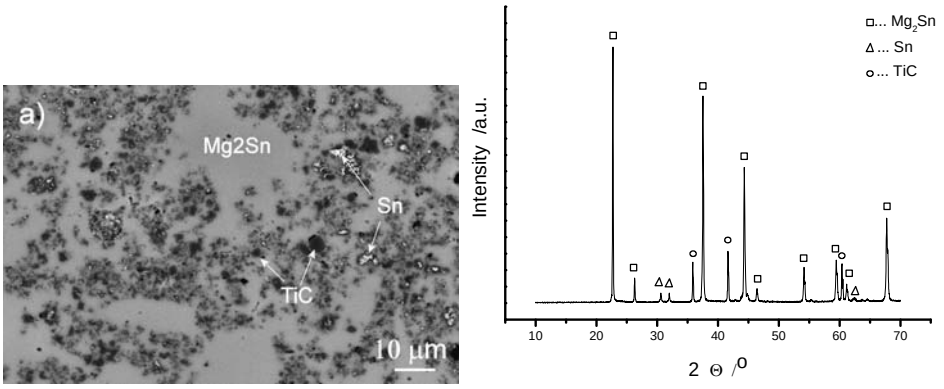

Fig. 7. a) SEM micrograph and b) XRD spectrum of pressurelessly sintered Mg_2Sn-Sn-$TiC_{(p)}$ composite sample with the initial composition 67 vol. %Mg_2Sn, 3 vol.% Sn and 30 vol.% TiC.

Regarding the mechanical properties of Mg-Mg_2Sn-TiC and Mg-Mg_2Sn-TiB_2 composite samples, which are summarized in Table 6, an increase in particulate content (Mg_2Sn and TiC or TiB_2) was observed to improve the Vickers hardness, while at the same time reducing the fracture toughness. In addition, the Vickers hardness of Mg-Mg_2Sn-TiC and Mg-Mg_2Sn-TiB_2 composite samples was found to be better than in the non-reinforced counterparts, while the fracture toughness was about 25% lower.

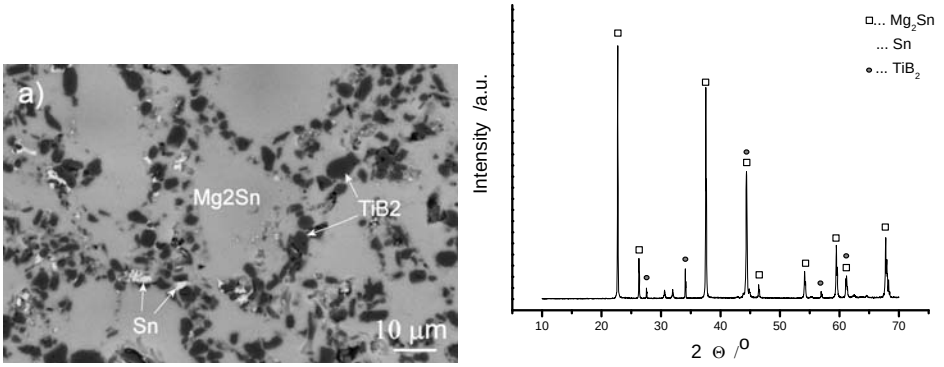

Fig. 8. a) SEM micrograph and b) XRD spectrum of pressurelessly sintered Mg_2Sn-Sn-$TiB_{2(p)}$ composite sample with the initial composition 67 vol. %Mg_2Sn, 3 vol.% Sn and 30 vol.% TiB_2.

Compared to the Al-Mg_2Sn-TiC or Al-Mg_2Sn-TiB_2 counterparts, the reduction of Vickers hardness is only slight. On the other hand, the fracture toughness of Mg-Mg_2Sn-TiC or Mg-Mg_2Sn-TiB_2 composites is almost twice as high as in their Al-Mg_2Sn-TiC or Al-Mg_2Sn-TiB_2 counterparts, which is due to the lamellar structure consisting of Mg_2Sn "Chinese script" in a matrix of magnesium.

Mg_2Sn-Sn-$TiC_{(p)}$, Mg_2Sn-Sn-$TiB_{2(p)}$ composites made by pressureless sintering

Pressureless sintering of green samples made either from as-milled Mg_2Sn powders of grade A and B, Table1, or mixed with various amounts of TiC or TiB_2 particles, resulted in dense composite specimens with a retained porosity of less than 5 vol. %. On the contrary, pressureless sintering of green samples made either from as-milled Mg_2Sn powder of grade C, Table1, or mixed with various amounts of TiC or TiB_2 particles, was found to be incomplete, with more than 10 vol. % of retained porosity.

The microstructure of sintered samples reinforced with ceramic particulates is presented in Figs. 7 and 8. The composites obtained consist of a continuous Mg_2Sn matrix and TiC or TiB_2 ceramic particulate reinforcement dispersed around the sintered Mg_2Sn grains and small Sn inclusions. In contrast, the microstructure of dense, non-reinforced samples was uniform, with fully sintered Mg_2Sn grains and Sn inclusions.

SEM-EDS evaluation of samples and XRD measurements imply that the Mg_2Sn-TiC and Mg_2Sn-TiB_2 systems are non-reactive, without secondary phases formed during sintering, and that sintering proceeded via non-reactive mechanism, assisted by the liquid Sn phase.

The mechanical properties of sintered samples are listed in Tables 7 and 8.

The Vickers hardness of pressurelessly sintered samples was found to be enhanced with an increasing amount of particulate reinforcement in the Mg_2Sn matrix, Table 2. This could be ascribed to an increased dislocation density in the microstructure and the presence of hard, brittle and essentially elastically deforming reinforcing phases in the Mg_2Sn matrix. In addition, Vickers hardness measurements also confirmed that sintering of samples with the same initial volume fraction of TiC or TiB_2 reinforcement resulted in composites with similar hardness. This is most probably caused by the similar microstructures of Mg_2Sn-TiC and Mg_2Sn-TiB_2composite samples, the same sintering mechanism and almost the same hardness of TiC and TiB_2 reinforcing particulates.

Table 7: Average room temperature Vickers hardness and fracture toughness of sintered Mg_2Sn -Sn-TiC samples.

Composite initial composition (wt. %)	Retained porosity (vol. %)	Density (g/cm^3)	Vickers hardness (GPa)	K_{IC} (MPa $m^{1/2}$)
97% Mg_2Sn (grade A)-3% Sn	4.8±0.5	3.7±0.2	1.0±0.1	1.7±0.2
87% Mg_2Sn (grade A)-3% Sn-10% TiC	3.5±0.4	3.8±0.2	1.4±0.1	1.4±0.1
68% Mg_2Sn (grade A)-2% Sn-30% TiC	4.3±0.4	4.1±0.4	1.5±0.2	1.0±0.1
49% Mg_2Sn (grade A)-1% Sn-50% TiC	4.9±0.5	4.3±0.5	1.8±0.2	0.7±0.1
95% Mg_2Sn (grade B)-5% Sn	3.1±0.3	3.8±0.5	0.9±0.1	1.8±0.2
86% Mg_2Sn (grade B)-4% Sn-10% TiC	2.7±0.3	3.8±0.3	1.0±0.1	1.4±0.1
66% Mg_2Sn (grade B)-3% Sn-30% TiC	3.9±0.4	3.9±0.4	1.3±0.1	1.1±0.1
48% Mg_2Sn (grade B)-2% Sn-50% TiC	4.1±0.5	4.1±0.5	1.7±0.2	0.6±0.1

Table 8: Average room temperature Vickers hardness and fracture toughness of sintered Mg_2Sn

Composite initial composition (wt. %)	Retained porosity (vol. %)	Density (g/cm^3)	Vickers hardness (GPa)	K_{IC} (MPa $m^{1/2}$)
97% Mg_2Sn (grade A)-3% Sn	4.8±0.5	3.7±0.2	1.0±0.1	1.7±0.2
87% Mg_2Sn (grade A)-3% Sn-10% TiB_2	3.5±0.4	3.8±0.2	1.5±0.1	1.3±0.1
68% Mg_2Sn (grade A)-2% Sn-30% TiB_2	4.3±0.4	4.1±0.4	1.7±0.2	0.8±0.1
49% Mg_2Sn (grade A)-1% Sn-50% TiB_2	4.9±0.5	4.3±0.5	1.9±0.2	0.6±0.1
95% Mg_2Sn (grade B)-5% Sn	3.1±0.3	3.8±0.5	0.9±0.1	1.8±0.2
86% Mg_2Sn (grade B)-4% Sn-10% TiB_2	2.7±0.3	3.8±0.3	1.0±0.1	1.4±0.1
66% Mg_2Sn (grade B)-3% Sn-30% TiB_2	3.9±0.4	3.9±0.4	1.6±0.1	1.0±0.1
48% Mg_2Sn (grade B)-2% Sn-50% TiB_2	4.1±0.5	4.1±0.5	2.0 ±0.2	0.5±0.1

Conclusions

1. The reactive synthesis of Mg_2Sn from the elements resulted in a high yield, single phase product with less than 0.2 wt. % of impurities (Mg or Sn), depending on the composition of the initial reactive mixture.
2. Additional crushing and subsequent milling of the reaction product (i.e. in a planetary mill) was found to be an easy operation, enabling cost-effective preparation of Mg_2Sn powders with an average particle size less than 5 μm, suitable for the production of Mg_2Sn-based advanced composites. Depending on the selected fabrication technique of (i) pressureless infiltration of porous Mg_2Sn, Mg_2Sn-TiC and Mg_2Sn-TiB_2 preforms with molten aluminium and magnesium, or (ii) pressureless sintering of green Mg_2Sn-TiC and Mg_2Sn-TiB_2 compacts, Mg_2Sn-based composites of different Mg_2Sn-TiC and Mg_2Sn-TiB_2 compacts, Mg_2Sn-based composites of different nature, microstructure and combination of properties were successfully prepared demonstrating the significant potential of Mg_2Sn phase as a composite matrix and of the particulate reinforcement.
3. Investigation of the effect of different microstructures developed in Mg_2Sn-based composites on their mechanical properties (hardness and toughness) revealed that Mg_2Sn as the line compound could be useful for tailoring an optimum combination of these properties.
4. The pressureless infiltration of porous Mg_2Sn, Mg_2Sn-TiC and Mg_2Sn-TiB_2 preforms with molten magnesium and aluminium resulted in dense (≥95 % T.D.) metal matrix composites with a metallic matrix discontinuously reinforced with Mg_2Sn and TiC or TiB_2 particulates. The infiltration proceeded spontaneously, without detectable chemical reactions between the preform skeleton and the molten infiltrants.
5. The composite samples infiltrated with molten magnesium possessed the characteristic lamellar ("Chinese script") eutectic microstructure, while in samples infiltrated with molten aluminium the appearance of fine Mg_2Sn-Sn

precipitates in an Al matrix mostly in the vicinity of the initially introduced Mg_2Sn particles has been observed.

6. In preforms with the addition of TiC or TiB_2 ceramic reinforcement, the microstructure development during infiltration occurred in the same way as in their non-reinforced counterparts. Because of the low temperature of preform infiltration (750 °C), the particulate reinforcements remained chemically inert in contact with molten magnesium or molten aluminium, resulting in a final microstructure of infiltrated composite samples the same as in non-reinforced counterparts. The only difference was observed inside the Al or Mg phases, which were completely reinforced with TiC or TiB_2 particles.
7. The microstructure of composite samples obtained by pressureless infiltration could be tailored to consist of a continuous aluminium or magnesium matrix, discontinuously reinforced with Mg_2Sn of different morphology (particulates in samples infiltrated with aluminium and the characteristic "Chinese script" eutectic phase in samples infiltrated with magnesium) and, when added, TiC or TiB_2 reinforcements. Such a microstructure design was projected in order to achieve an optimum combination of enhanced fracture toughness (particularly improved by the "Chinese script" phase appearing in samples infiltrated with magnesium), with tensile properties and a hardness superior to that of conventional Mg-Sn alloys.
8. The Vickers hardness was found to be better in samples infiltrated with aluminium than in counterparts infiltrated with magnesium. On the other hand, quite the opposite behaviour was found regarding fracture toughness. Due to their characteristic lamellar structure consisting of Mg_2Sn as "Chinese script" in the matrix, composite samples infiltrated with magnesium possessed an extraordinary fracture toughness almost twice as that of the counterparts infiltrated with aluminium, in which the Mg_2Sn phase appeared as particulates. Within each single group of infiltrated samples (i.e. samples with the same *qualitative* composition), the Visckers hardness was enhanced while the fracture toughness decreased with increasing total amount of particulate reinforcement.
9. Pressureless sintering of green samples made from Mg_2Sn powders with 3-5% of free Sn, or from mixtures of these powders with various amounts of TiC or TiB_2 particles, resulted in dense composite specimens with a retained porosity less than 5 vol. %. On the contrary, pressureless sintering of green samples made from Mg_2Sn powder without free Sn or a mixture of the same powder with various amounts of TiC or TiB_2 particles was found to be incomplete, with more than 10 vol. % of retained porosity.
10. The composites obtained consisted of a continuous Mg_2Sn matrix and TiC or TiB_2 ceramic particulate reinforcement dispersed around the sintered Mg_2Sn grains and small Sn inclusions. In contrast, the microstructure of dense, non-reinforced samples was uniform, with fully sintered Mg_2Sn gains and Sn inclusions.
11. During sintering, the formation of secondary phases was not observed. Densification of composite samples proceeded by non-reactive sintering, assisted by molten tin.

12. The Vickers hardness of sintered samples (intermetallic matrix composites with a Mg_2Sn matrix discontinuously reinforced with TiC or TiB_2 ceramic reinforcement) was significantly improved in comparison with metal matrix composites obtained by infiltration. The exception was fracture toughness, which in sintered samples was reduced to approximately one third or even one quarter of the values measured in metal matrix composites obtained by infiltration.
13. With densities higher than the density of aluminium and magnesium alloys, Mg_2Sn-based composites have a limited potential for weight reduction of structural parts. However, some of the Mg_2Sn composites (especially Mg-Mg_2Sn metal matrix composites) could offer a unique combination of properties, including the ability of the composite microstructure (lamellar, consisting of Mg_2Sn "Chinese script" in a magnesium solid solution) to develop a toughening mechanism in combination with improved tensile properties and hardness.

Acknowledgement

This work was supported by funding from the Public Agency for Research and Development of the Republic of Slovenia, as well as the Impol Aluminium Company and Bistral d.o.o. from Slovenska Bistrica, Slovenia, contract No. 1000-07-219308.

References

[1] N. Hort, Y. Huang, T. A. Leil, P. Maier, K. U. Kainer, Adv. Eng. Mat., 8(5), 2006; pp. 359.
[2] N.Hort, Y. Huang, K. U. Kainer, F. Moll, K. U. Kainer, Adv. Eng. Mat., 8(4), 2006; pp. 235.
[3] J. Gröbner, A. Janz, A. Kozlov, Dj. Mirković, R. S. Fetzer, JOM, 60(12), 2009; pp. 32.
[4] M. Zhang, W. Z. Zhang, G. Z. Zhu, Scrpita Materialia 59, 2008; pp. 866.
[5] Z. Min, Z. W. Zheng, Z. G. Zhen, Y. Kun, Trans. Nonferrous Met. China 17; 2007; pp. 1428.
[6] Z.X. Ping, C.Y. Gui, X.Y. HUa, Trans Nonferrous Met.Soc.China 18, 2008; 299.
[7] B. H. Kim, J. J. Jeon, K. C. Park, B. G. Park, Y. H. Park, I. M. park, Archives of Materials Science and Engineering, 30(2), 2008; pp.93.
[8] S. Koch, H. Antrekowitsch, BHM, 153(7), 2008; pp. 278.
[9] O. Madelung, U. Rössler, M. Schulz, In Non-Tetrahedrally Bonded Elements and Binary Compounds I, Springer-Verlag, 1998; pp. 1-3.
[10] C. Zhang, P. Han, X. Yan, C. Wang, L. Xia, B. Xu, J. Phys. D: Appl. Phys., 42, 2009; pp. 1. (doi: 125403).
[11] W. Y. Feng, D. W. Bo, Z. T. Young, Trans. Nonferrous Met. Soc. China, 19 2009; pp. 1196.
[12] K. Kondoh, H. Oginuma, T. Aizawa, Materials Transactions, 42, 2001; pp.1293
[13] K. Niihara, R. Morena, D. P. Hasselman, J. Mater. Sci. Lett. 1, 1982; pp. 13.
[14] A. A. Nayeb-Hasemi, J. B. Clark, J. Bull. Alloy Phase Diagrams 63, 1984; 467.